DOI: 10.1002/chem.200701766

A Mixed-Valence, Hexadecamolybdenum Cluster With an Mo^{VI} Cubane "Jewel" in a "Setting" of Five Molybdate^{VI}-Linked Dinuclear Mo^{V} Units

Lyndal M. R. Hill, Brendan F. Abrahams, and Charles G. Young*[a]

Abstract: The hexadecanuclear, mixed-valence cluster $[Mo_{16}O_{42}(OH)_2(3\text{-}i\text{Pr}C_3H_3N_2)_{12}]\cdot n\,H_2O$ (**1**), has been synthesized and characterized by X-ray crystallography, IR spectroscopy and mass spectrometry. The C_2-symmetric complex consists of a cubane $Mo^{VI}{}_4O_4$ "jewel" held in a 10-point "setting" comprised of five dinuclear Mo^{V} units tethered together by two tetrahedral Mo^{VI} centers. The dinuclear units are ligated by twelve 3-isopropylpyrazole units that interact with the Mo–O framework through a network of hydrogen bonds. Structural parameters, charge requirements, and bond valence sum analyses support the assignment of +5 and +6 oxidation states to the dinuclear and cubane/tetrahedral Mo centers, respectively. Space filling models reveal that the pyrazole groups coat much of the surface of the molecule, apart from a number of oxo-rich seams that trace a chiral pattern across the surface. Complex **1** exhibits a unique structure that combines moieties generally atypical of polyoxometalates, viz., a Mo cubane containing only two terminal oxo ligands, and three distinct $Mo^{V}{}_2$ units (including a 5-coordinate Mo center) tethered into a 10-point "setting" by tetrahedral Mo^{VI} centers.

Keywords: cluster compounds · molybdenum · polyoxometalates · self-assembly · structure elucidation

Introduction

Polyoxometalates are well known in early transition metal chemistry and many have found applications in analytical chemistry, materials science, nanotechnology, homo- and heterogeneous catalysis, green chemistry, environmental remediation, and medicine.[1–3] These complexes vary in nuclearity, charge, size, and topology, and the variation of these attributes provides enormous opportunities for new structures, properties, and applications; the influence of topology on the properties of polyoxometalate species is of particular interest to researchers in this area.

Isopolyanions and Keggin, Dawson, and lacunary species are classic examples of polyoxometalates in the small size range.[4] Cation-anion aggregates, e.g., Weakley complexes, constitute medium-sized species.[4] Extremely large composite and mesoscopic polyoxometalates have been pioneered by Müller and co-workers;[5,6] these complexes are now being fabricated into nanostructured materials with exciting properties and applications. Very few polyoxomolybdates feature tetrahedral molybdate (MoO_4^{2-}) units and those that do typically contain a second metal (Cu, Ni, Co) bound at multiple peripheral sites.[7–10] Only two of these species contain dinuclear Mo^{V} fragments, viz., a spherical Mo_{13} porous capsule[11] and an approximately tetrahedral Mo_{13} complex.[12] To date, examples of hexadecamolybdates are limited to the "shrink-wrapped" anion $[H_2Mo_{16}O_{52}]^{10-}$,[13] and the "cation-encapsulating" anions $[H_2Mo_{16}(OH)_{12}O_{40}]^{6-}$ and $[NaMo_{16}(OH)_{12}O_{40}]^{7-}$.[14,15] These mixed-valence species possess spherical topologies and are devoid of tetrahedral centers.

Here, we report the synthesis and structure of $[Mo_{16}O_{42}(OH)_2(3\text{-}i\text{Pr}C_3H_3N_2)_{12}]\cdot n\,H_2O$ (**1**), formed upon the degradation of $[Tp^{i\text{Pr}}MoO_2\{OC_6H_3(OMe)_2\text{-}2,3\}]$ ($Tp^{i\text{Pr}}$ = hydrotris(3-isopropylpyrazolyl)borate) in dichloromethane/methanol mixtures. The non-spherical, electrically neutral, mixed-valence cluster is comprised of fragments that are generally atypical of polyoxometalates and features a network of hydrogen bonds between the surface pyrazole NH and framework oxygen atoms.

[a] Dr. L. M. R. Hill, Dr. B. F. Abrahams, Prof. C. G. Young
School of Chemistry, University of Melbourne
Parkville, Victoria 3010, Australia
Fax: (+61) 3-9347-5180
E-mail: cgyoung@unimelb.edu.au

Supporting information for this article is available on the WWW under http://www.chemeurj.org/ or from the author.

Results and Discussion

Views of the complete structure (excluding lattice solvent) and a polyhedral representation of **1** are shown in Figure 1a–c, and a view of the central donor-atom/metal framework is given in Figure 2. The C_2-symmetric complex consists of a cubane "jewel" held in a 10-point "setting" comprised of five dinuclear units tethered together by two tetrahedral Mo centers (Figure 1a). The periphery of the cluster is decorated by isopropylpyrazole ligands, H-bonded to oxo ligands and lattice water molecules, the H-bonding network being displayed in Figure 1b.

The cubane unit consists of two $Mo_2(\mu_3\text{-O-donor})_2$ butterfly units, linked via four Mo–O bonds. The Mo atoms of the top face, Mo1 and Mo1′, are further coordinated by a terminal oxo group (1.710(5) Å) and two μ_2-oxo ligands from adjacent dinuclear units. The Mo atoms on the lower face, Mo2 and Mo2′, are bound by three μ_2-oxo ligands from three separate dinuclear units. The faces of the cubane also deviate from planarity. The cubane core and the coordinated terminal and μ_2-oxo groups can be described in terms of four edge shared MoO_6 octahedra, the structure being reminiscent of $[W_4O_{16}]^{8-}$ and certain subunits in polyoxometalates.[4] Bond distances within the cubane unit are given in Table 1. Table 2 lists the bond and torsion angles and Table 3 lists the interplanar angles calculated for the cubane unit. The Mo···Mo distances in the cubane unit of **1** exceed 3.4 Å, consistent with the presence of Mo^{VI} centers. The cubane unit of **1** is a rare example of an asymmetric Mo_4O_4-cluster, featuring terminal oxo ligands at only two of the four Mo centers, and a complement of μ_3-bridging oxo and hydroxo ligands. To date, only four Mo^{VI}[16] and four Mo^{V}[17] cubane complexes have been structurally characterized.

The cubane "jewel" is clasped within a 10-point "setting" comprised of five dinuclear *syn*-$[Mo_2O_2(\mu\text{-O})_2]^{2+}$ units linked by two tetrahedral molybdate(VI) units, and decorated by peripheral 3-isopropylpyrazole ligands (Figure 1a,b). The bond distances within the dinuclear units are listed in Table 4. The relevant Mo centers possess distorted-octahedral geometries, with the exception of Mo5 and Mo5′, which have square pyramidal geometries (Figures 1c (green centers) and 2). The axial terminal oxo groups of the dinuclear units point away from the center of the molecule. The dinuclear units are of three types. Two of the dinuclear units (Mo3/Mo4 and Mo3′/Mo4′) bind across opposing lateral faces of the cubane via axial μ-oxo ligands (viz., *trans* to oxo ligands O5 and O14); one Mo bears two pyrazole ligands, and the other is coordinated by a single pyrazole. Two other dinuclear units bind across the other lateral faces of the cubane, via μ-oxo ligands that occupy the equatorial positions of Mo5 and Mo5′; the second Mo atom in these units, Mo6 and Mo6′, bind two pyrazole ligands. Finally, a unique dinuclear unit (Mo7/Mo7′) binds the bottom face of the cubane via its axial μ-oxo ligands (viz., *trans* to oxo ligands O20 and O20′), with the Mo centers bearing *anti* pyrazole ligands.

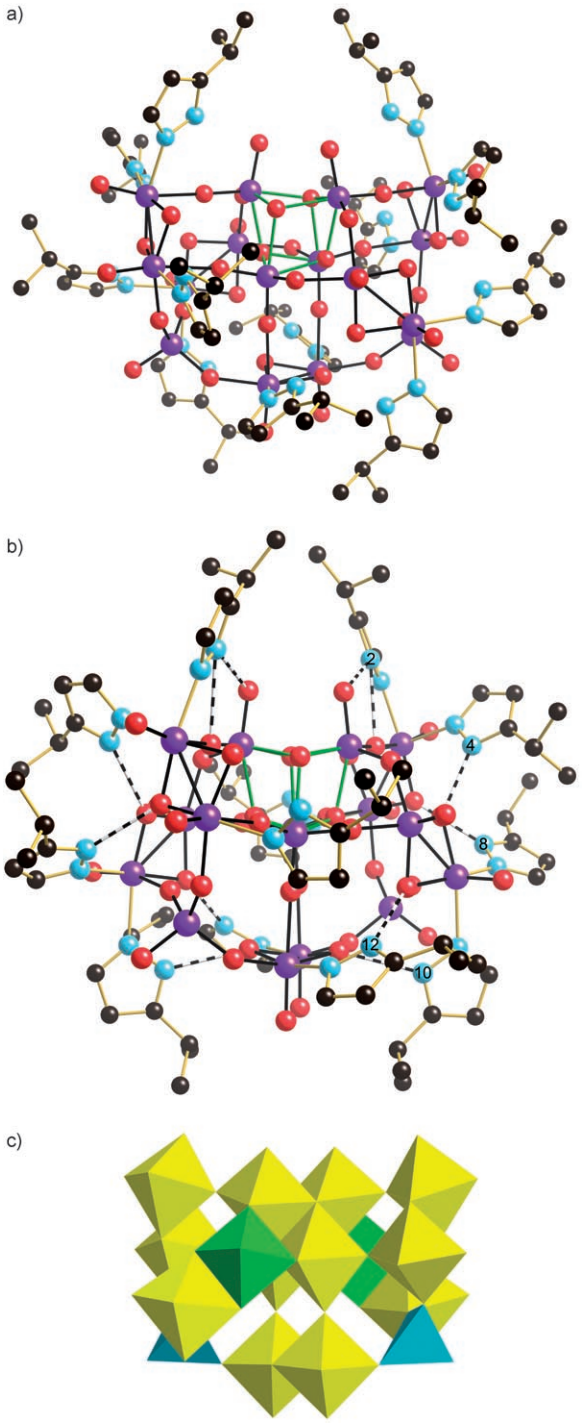

Figure 1. a) Structure of **1** (Mo purple; O red; N blue; C black). The C_2 axis runs vertically. Apart from the cubane (linkages in green), the Mo–O framework is represented with black bonds. All other bonds are gold. b) The H-bonding network in **1**. H-bonds are indicated by black and white rods, with participating nitrogen centers numbered. The molecule has been rotated by ≈45 ° about the C_2 axis with respect to the image in (a). c) Polyhedral representation of **1**. The six-, five- and four-coordinate centers are shown in yellow, green and blue, respectively.

The terminal oxo ligands possess characteristically short Mo–O distances (≈1.67 Å), while the Mo–(μ-O) distances fall into two ranges: 1.9–2.0 Å for the single bonds linking

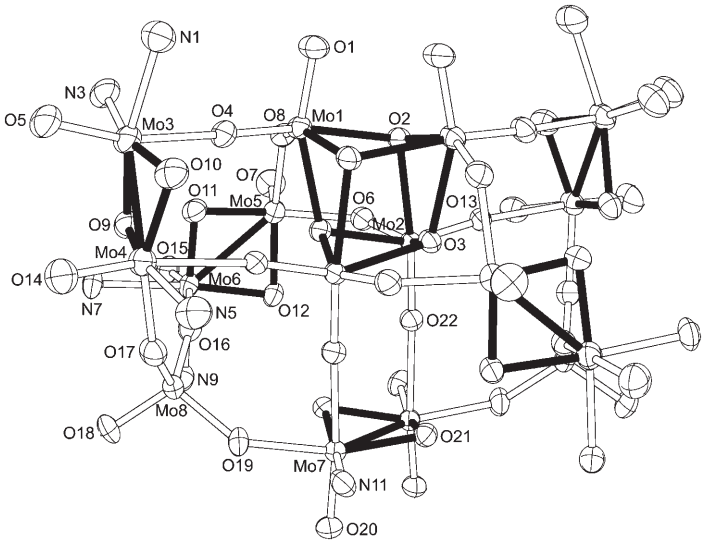

Figure 2. ORTEP projection of the donor-atom/metal framework of **1** (50% thermal ellipsoids). Dark bonds highlight the cubane and dinuclear moieties. The tetrahedral Mo sites (Mo8/Mo8′) lie at the lower left and right of the diagram.

dinuclear cores, and 2.0–2.3 Å for weaker cubane/dinuclear-unit interactions. The bond distances and angles in the dinuclear fragments conform with those expected of $[Mo^{V}_{2}O_{2}(\mu\text{-}O)_{2}]^{2+}$ units possessing a single Mo–Mo bond.[18]

Each of the two tetrahedral Mo centers, Mo8/Mo8′, is linked to three different dinuclear units via μ_2-oxo ligands. Their coordination spheres are completed by a terminal oxo ligand, projecting away from the cubane unit. These molybdate units occupy *anti*, equatorial sites of the basal dinuclear unit. Bond distances and angles for these tetrahedral centers are provided in Table 5. The Mo8/8′–(μ-O) bonds are ≈0.06–0.10 Å longer than the terminal oxo bond (Mo8-O18) of 1.705(5) Å, and all are typical of four-coordinate Mo^{VI} centers. The bond angles subtended at Mo8/8′ (107.3(3)-111.3(2)°) are all close to the tetrahedral angle.

Twelve, H-bonded 3-isopropylpyrazole ligands decorate the periphery of the complex (Figure 1b). The two uppermost pyrazole ligands are H-bonded to the terminal oxo ligands on the cubane (N2H···O1 = 2.888(9) Å), and the μ_2-oxo link provided by O4 (N2H···O4 = 2.880(9) Å). The μ_2-oxo link of O21 is also H-bonded, with N10H···O21′ = 2.686(8) Å. Six of the remaining eight ligands participate in NH···O H-bonding interactions with bridging oxo ligands of the $Mo_2O_2(\mu\text{-}O)_2$ units, with H-bond distances ranging from 2.722(9)–2.741(8) Å. Donor atom N6 is H-bonded to the water of crystallization, O24 and O25. Thus, each of the pyrazole ligands is bound as a neutral, H-bonded moiety. There are no counterions in the lattice and hence the complex is electrically neutral.[19] Space-filling models of the complex reveal that the pyrazole groups coat much of the surface, apart from a number of oxo-rich seams that trace out a chiral pattern (see the Supporting Information).

Structural parameters (vide supra) and charge balance requirements support the assignment of +5 and +6 oxidation

Table 1. Bond distances in the Mo_4O_4 cubane core.

Bond or atom pair	Distance [Å]	Bond or atom pair	Distance [Å]
O2···O23	2.421(17)	Mo2–O2	2.356(5)
Mo1–O1	1.710(5)	Mo2–O3	1.975(5)
Mo1–O2	2.218(5)	Mo2–O3′	2.207(5)
Mo1–O2′	2.084(5)	Mo2–O6	1.818(5)
Mo1–O3′	2.243(5)	Mo2–O13	1.726(5)
Mo1–O4	1.769(5)	Mo2–O22	1.736(5)
Mo1–O8	1.811(5)		

Table 2. Bond and torsion angles of the Mo_4O_4 cubane core.

Atoms	Angle [°]	Atoms	Angle [°]
Mo1–O2–Mo1′	104.0(2)	Mo2–O3′–Mo2′	101.0(2)
O2–Mo1–O2′	73.2(2)	O3′–Mo2′–O3	73.3(2)
Mo1–O2–Mo1′–O2′	−17.4(3)	Mo2–O3′–Mo2′–O3	−24.0(2)
O2–Mo1–O2′–Mo1′	−18.6(3)	O3′–Mo2′–O3–Mo2	27.1(3)
O2–Mo1–O3′	71.4(2)	Mo1–O2′–Mo2′	100.3(2)
Mo1–O3′–Mo2	110.9(2)	O2′–Mo2′–O3′	72.4(2)
O3′–Mo2–O2	69.5(2)	Mo2′–O3′–Mo1	107.9(2)
Mo2–O2–Mo1	106.5(2)	O3′–Mo1–O2′	73.0(2)
O2–Mo1–O3′–Mo2	10.6(2)	Mo1–O2′–Mo2′–O3′	−19.9(2)
Mo1–O3′–Mo2–O2	−10.1(2)	O2′–Mo2′–O3′–Mo1	19.1(2)
O3′–Mo2–O2–Mo1	9.9(2)	Mo2′–O3′–Mo1–O2′	−21.6(2)
Mo2–O2–Mo1–O3′	−9.6(2)	O3′–Mo1–O2′–Mo2′	17.4(2)

Table 3. Interplanar angles of the Mo_4O_4 cubane.

Face	Plane 1	Plane 2	Angle [°]
upper	O2–Mo1′–O2′	O2–Mo1–O2′	22.0(1)
	Mo1′–O2–Mo1	Mo1–O2′–Mo1′	28.7(2)
lower	O3′–Mo2′–O3	O3′–Mo2–O3	32.0(1)
	Mo2–O3′–Mo2′	Mo2′–O3–Mo2	40.6(2)
side A	O2–Mo1–O3′	O3′–Mo2–O2	11.7(3)
	Mo1–O3′–Mo2	Mo2–O2–Mo1	16.4(3)
side B	Mo1–O2′–Mo2′	Mo2′–O3′–Mo1	31.2(2)
	O2′–Mo2′–O3′	O3′–Mo1–O2′	23.7(2)
combinations[a]	lower	upper	0.00(1)
	side A	upper or lower	88.5(1)
	side B	upper or lower	90.0(1)
	side A	side B	88.8(2)

[a] Plane 1 and Plane 2 refer to the average planes calculated for the four-membered faces listed.

Table 4. Bond distances in the $Mo_2O_2(\mu\text{-}O)_2$ groups.

Bond	Atoms	Distance [Å]	Bond	Atoms	Distance [Å]
Mo–Mo	Mo3–Mo4	2.5618(11)	Mo–O[a]	Mo3–O9	1.937(5)
	Mo5–Mo6	2.5871(10)		Mo3–O10	1.940(6)
	Mo7–Mo7′	2.5659(14)		Mo4–O9	1.941(5)
Mo=O	Mo3–O5	1.668(6)		Mo4–O10	1.930(6)
	Mo4–O14	1.677(6)		Mo5–O11	1.926(5)
	Mo5–O7	1.663(6)		Mo5–O12	1.925(5)
	Mo6–O15	1.674(6)		Mo6–O11	1.932(5)
	Mo7–O20	1.669(5)		Mo6–O12	1.951(5)
Mo–O[b]	Mo3–O4	2.183(5)		Mo7–O21	1.940(5)
	Mo4–O13′	2.299(5)		Mo7–O21′	1.923(5)
	Mo4–O17	2.037(5)	Mo–N	Mo3–N1	2.184(7)
	Mo5–O6	2.027(5)		Mo3–N3	2.211(7)
	Mo5–O8	2.030(5)		Mo4–N5	2.176(7)
	Mo6–O16	2.165(5)		Mo6–N7	2.217(6)
	Mo7–O22′	2.269(5)		Mo6–N9	2.210(6)
	Mo7–O19	2.073(5)		Mo7–N11	2.203(6)

[a] Atoms in dinuclear units. [b] Atoms in core framework.

Table 5. Bond distances and angles at the tetrahedral Mo sites, Mo8 and Mo8′.

Bond	Distance [Å]	Oxygen Type	Connectivity	Angle [°]
			O16–Mo8–O17	110.2(3)
Mo8–O16	1.761(5)	bridge to Mo6	O16–Mo8–O18	109.0(3)
Mo8–O17	1.801(5)	bridge to Mo4	O16–Mo8–O19	111.3(2)
Mo8–O18	1.705(5)	terminal oxo	O17–Mo8–O18	108.5(3)
Mo8–O19	1.790(5)	bridge to Mo7	O17–Mo8–O19	110.4(3)
			O18–Mo8–O19	107.3(3)

states to the dinuclear and cubane/tetrahedral Mo centers, respectively. These oxidation state assignments were confirmed by bond valence sum (BVS) analyses. The BVS approach establishes the bond valence of each bond in a compound, enabling a BVS to be calculated for a given atom, as simply the additive effect of the contributing bonds. Equation (1) defines the relationship between the bond length, r, and bond valence, s, for a cation-anion pair:[20]

$$s = \exp\left[(r_o - r)/B\right] \quad (1)$$

In which r_o and B are empirically determined parameters. The oxidation state of the cation (i), V_i, can then be estimated using Equation (2) (where s_{ij} is the bond valence between the atoms i and j).

$$V_i = \sum_j s_{ij} \quad (2)$$

Oxidation-state-specific r_o values have been established for Mo^V and Mo^{VI} bonds to O and N.[21] More precise oxidation states may be calculated using oxidation-state-specific values.[22] Liu and Thorp claim to obtain reliable BVS values only when their values of r_o are used.[21] Table 6 provides r_o values for the pertinent bonds of the Mo_{16} complex.

In order to apply the r_o values in Table 6 to the Mo_{16} complex, the cubane and tetrahedral sites (Mo1, Mo2 and Mo8) were assigned as Mo^{VI} centers and the dinuclear sites (Mo3, Mo4, Mo5, Mo6 and Mo7) as Mo^V. The results of bond valence sums carried out using Equations (1) and (2) are given in Table 7.

The BVS calculations vary somewhat depending on the set of r_o values used. The upper entries of Table 7 support a +6 oxidation state assignment for the cubane and tetrahedral Mo atoms, while the lower entries provide reasonable values supporting dinuclear Mo^V centers. Successful reports of the application of bond valence sums to molybdenum polyanions containing Mo^V–Mo^V bonds have not indicated which of the r_o values tabulated by Brown were used.[13,30] Thus, the BVS approach supports the oxidation state assignments for **1**, though it is recognized that the selective use of r_o values (here, the combining of the two sets of results in Table 6) is a consequence of the prevailing accounts of different bond valence parameters (namely r_o). In conclusion, the above BSV analysis supports the formulation of the complex as a neutral $Mo^V_{10}Mo^{VI}_6$ mixed-valence species.

The diamagnetic, EPR-silent complex exhibits medium intensity IR ν(Mo=O) bands at $\approx$950 cm^{-1} and ν(Mo–μ-O) and ν(Mo(μ-O)$_2$) bands at $\approx$897–827 cm^{-1}, 740–728 cm^{-1} and 478 cm^{-1}. Broad, weak bands at 3241 and 3133 cm^{-1} are

Table 6. Reported r_o values for molybdenum.

Bond	r_o [Å][a]
Mo^{II-VI}–O	1.882[23]
Mo^{V-VI}–O	1.872[24]
Mo^{III-VI}–O	1.890[25]
Mo^{VI}–O	1.882,[26] 1.90,[27] 1.907[21]
Mo^V–O	1.917[21]
Mo^V–N	1.893,[28] 2.006[21]

[a] Apart from the values of Liu and Thorp[21] all values have been tabulated by Brown.[29]

Table 7. BVS calculations for **1**.

Mo site	Mo1	Mo2	Mo8	Mo3	Mo4	Mo5	Mo6	Mo7
BVS[a]	5.91	6.06	5.91	5.53	5.53	5.42	5.45	5.51
	5.80	5.95	5.80	4.91	5.02	5.04	4.85	5.01

[a] The upper entries use r_o values reported by Liu and Thorp[21] and the lower entries use values tabulated by Brown (r_o: Mo^{VI}–O 1.90; Mo^V–O 1.89; Mo^V–N 1.893; see Table 6).[29] B is taken to be 0.37.[20]

assigned to the ν(NH) modes of the pyrazole units. The positive ion electrospray ionization mass spectrum (ESI-MS) of **1** in MeCN/MeOH exhibited a strong peak cluster around *m/z* 1810–1825 (see the Supporting Information). Half-integer peak separations were consistent with a dicationic parent ion peak cluster, principally solvated $[\mathbf{1}+2H]^{2+}$. Peaks resulting from successive loss of five isopropylpyrazole units were also observed. The compound was not sufficiently soluble to allow NMR experiments.

Conclusion

A hexadecanuclear $Mo^{V}_{10}Mo^{VI}_{6}$ species (**1**) stabilized by a H-bonded network of surface 3-isopropylpyrazole ligands has been isolated and structurally characterized. Electrically neutral, mixed-valent **1** exhibits a unique structure that combines moieties generally atypical of polyoxometalates, viz., the first Mo cubane "jewel" to contain only two terminal oxo ligands[19] and three distinct Mo^{V}_{2} units (including a 5-coordinate Mo center) tethered into a 10-point "setting" by two tetrahedral Mo^{VI} centers.

Experimental Section

Syntheses:

[Tp^{iPr}MoO$_2${OC$_6$H$_3$(OMe)$_2$-2,3}]: The complex was prepared by adapting a literature procedure described by Millar et al.[31,32] A solution of [Tp^{iPr}MoO$_2$Cl] (1.00 g; 2 mmol), 2,3-dimethoxyphenol (5 mmol) and triethylamine (3–4 mL; 21.5–28.7 mmol) in dichloromethane (30 mL) was stirred for 3 days, whereupon the reaction mixture was reduced to low volume ($\approx$5 mL) by rotary evaporation. The residue was purified by column chromatography on silica gel by using dichloromethane as eluent. The complex eluted as an orange band after unreacted [Tp^{iPr}MoO$_2$Cl] and excess parent phenol. The isolated fraction was reduced to dryness, then treated with methanol and refrigerated to yield crystals (yield 1.10 g, 90%).

^{1}H NMR (C$_6$D$_6$, 400 MHz, 23°C): δ = 1.00, 1.20, 1.23 (3×d, 6H; 6×CH$_3$ of *i*Pr), 3.33, 3.78 (2×s, 3H; 2×OCH$_3$), 3.98 (sept, 2H; CH of *i*Pr), 4.83 (sept, 1H; CH of *i*Pr), 5.66 (d, 1H; 4-CH of Tp^{iPr}), 5.87 (d, 2H; 4-CH of Tp^{iPr}), 6.24 (dd, 1H; arene ring CH), 6.28 (dd, 1H; arene ring CH), 6.61 (t, 1H; arene ring CH), 7.19 (d, 1H; 5-CH of Tp^{iPr}), 7.36 ppm (d, 2H; 5-CH of Tp^{iPr}); IR (KBr): $\tilde{\nu}$ = 2503 (m, BH), 2466 (w, BH), 1507 (s, CN), 925 (s, MoO$_2$), 903 cm^{-1}(s, MoO$_2$); elemental analysis calculated (%) for C$_{26}$H$_{37}$BMoN$_6$O$_5$: C 50.34, H 6.01, N 13.55; found: C 49.79, H 5.85, N 13.16.

*Complex **1***: The instability of [Tp^{iPr}MoO$_2${OC$_6$H$_3$(OMe)$_2$-2,3}] and related dioxo complexes in the absence of excess phenolate co-ligand has been noted[32] and di-, tetra-, octa- and hexadecanuclear (**1**) species are formed upon degradation under different conditions.

Attempts to grow crystals of [Tp^{iPr}MoO$_2${OC$_6$H$_3$(OMe)$_2$-2,3}] by diffusion of methanol into a solution of the complex in dichloromethane led to the development of a blue coloration and large ruby-red crystals of **1** ($\approx$10% yield) after two weeks. IR (KBr disk): $\tilde{\nu}$ = 3241 (w, NH), 3133 (w, NH), 2967 (m), 2933 (w), 2873 (w), 1369 (w-m), 957 (m, Mo=O), 947 (m, Mo=O), 897 (s, Mo−μ-O), 876 (s, Mo−μ-O), 860 (s, Mo−μ-O), 827 (s, Mo−μ-O), 740 (m, Mo(μ-O)$_2$), 728 (m), 478 cm^{-1} (w-br). The compound was not obtained in sufficient yield to permit elemental analysis.

Crystal data: Complex **1** (n = 4.94): C$_{72}$H$_{131.89}$Mo$_{16}$N$_{24}$O$_{48.94}$, M_r = 3652.02, monoclinic, space group *C*2/*c*, a = 24.608(4), b = 19.517(3), c = 30.086(5) Å, β = 107.002(3)°, V = 13818(4) Å^3, Z = 4, ρ_{calcd} = 1.751 g cm^{-3}, $\mu(Mo_{K\alpha})$ = 14.74 cm^{-1}, T = 293 K, $2\theta_{max.}$ = 53.42°, 39569 measured reflections, 14275 independent reflections all of which were used in the refinement, $R1$ [$I > 2\sigma(I)$] = 0.0614, $wR2$ (all data) = 0.1612. Data were collected by using a Bruker CCD diffractometer. The structure was solved by direct methods, and refined by a full-matrix least-squares procedure.[33]

The asymmetric unit contains an Mo_8 fragment; the Mo_{16} cluster, **1**, is generated by the crystallographic 2-fold symmetry. The Mo centers and their donor atoms are well defined and free of disorder. The six 3-isopropylpyrazole ligands of the asymmetric unit were modeled using SAME restraints in order to provide reasonable thermal parameters for the anisotropic ring atoms. Two isopropyl groups required isotropic modeling for rotationally-related forms, owing to the considerable thermal motion.

Solvent molecules (water) were refined as isotropic atoms. A total of four solvent sites were identified. A water molecule with full occupancy, O23, is H-bonded to O2 of the cubane. Two water molecules (O24 and O25) are involved in H-bonding with a pyrazole nitrogen (N6), with O25 and the nearby O50 having complementary site occupancies ($\approx$47%) to O24 ($\approx$53%). The crystal lattice may contain additional solvent in channel/s, as evidenced by the presence of a small solvent accessible void that could accommodate approximately one water molecule per asymmetric unit ($\approx$1% volume). Hydrogen atoms were not assigned to the solvent sites.

CCDC 626899 (**1**) contains the supplementary crystallographic data for this paper. These data can be obtained free of charge from The Cambridge Crystallographic Data Centre via www.ccdc.cam.ac.uk/data_request/cif

Acknowledgements

We thank Ms. Sally Duck for mass spectrometric data and gratefully acknowledge the financial support of the University of Melbourne, the Australian Research Council, and the donors of the Petroleum Research Fund (administered by the American Chemical Society).

[1] *Polyoxometalates: From Platonic Solids to Anti-Retroviral Activity* (Eds.: M. T. Pope, A. Müller), Kluwer Academic Publishers, Dordrecht, **1994**.

[2] *Polyoxometalate Chemistry from Topology via Self-Assembly to Applications*, (Eds.: M. T. Pope, A. Müller), Kluwer Academic Publishers, Dordrecht, **2001**.

[3] C. L. Hill in *Comprehensive Coordination Chemistry II, Vol. 4* (Eds.: J. A. McCleverty, T. J. Meyer), Pergamon-Elsevier, Amsterdam, **2004**, pp. 679–759.

[4] M. T. Pope in *Comprehensive Coordination Chemistry II, Vol. 4* (Eds.: J. A. McCleverty, T. J. Meyer), Pergamon-Elsevier, Amsterdam, **2004**, pp. 635–678.

[5] a) A. Müller, P. Kögerler, H. Bögge, *Struct. Bonding (Berlin)* **2000**, *96*, 203–236; b) A. Müller, P. Kögerler, C. Kuhlmann, *Chem. Commun.* **1999**, 1347–1358; c) A. Müller, C. Serain, *Acc. Chem. Res.* **2000**, *33*, 2–10.

[6] L. Cronin in *Comprehensive Coordination Chemistry II, Vol. 7* (Eds.: J. A. McCleverty, T. J. Meyer), Elsevier Pergamon, Amsterdam, **2004**, pp. 1–56.

[7] D. Hagrman, C. Zubieta, D. J. Rose, J. Zubieta, R. C. Haushalter, *Angew. Chem.* **1997**, *109*, 904–907; *Angew. Chem. Int. Ed.* **1997**, *36*, 873–876.

[8] D. Hagrman, C. Sangregorio, C. J. O'Connor, J. Zubieta, *J. Chem. Soc. Dalton Trans.* **1998**, 3707–3710.

[9] W. Yang, C. Lu, H. Zhuang, *J. Chem. Soc. Dalton Trans.* **2002**, 2879–2884.

[10] E. Burkholder, J. Zubieta, *Inorg. Chim. Acta* **2005**, *358*, 116–122.

[11] A. Müller, L. Toma, H. Bögge, C. Schäffer, A. Stammler, *Angew. Chem.* **2005**, *117*, 7935–7939; *Angew. Chem. Int. Ed.* **2005**, *44*, 7757–7761.

[12] H. K. Chae, W. G. Klemperer, D. E. Páez Loyo, V. W. Day, T. A. Eberspacher, *Inorg. Chem.* **1992**, *31*, 3187–3189.
[13] D.-L. Long, P. Kögerler, L. J. Farrugia, L. Cronin, *Angew. Chem.* **2003**, *115*, 4312–4315; *Angew. Chem. Int. Ed.* **2003**, *42*, 4180–4183.
[14] M. I. Khan, A. Müller, S. Dillinger, H. Bögge, Q. Chen, J. Zubieta, *Angew. Chem.* **1993**, *105*, 1811–1814; *Angew. Chem. Int. Ed.* **1993**, *32*, 1780–1782.
[15] M. I. Khan, Q. Chen, J. Salta, C. J. O'Connor, J. Zubieta, *Inorg. Chem.* **1996**, *35*, 1880–1901.
[16] a) J. Glerup, A. Hazell, K. Michelsen, *Acta Chem. Scand.* **1991**, *45*, 1025–1031; b) Y. Hayashi, K. Toriumi, K. Isobe, *J. Am. Chem. Soc.* **1988**, *110*, 3666–3668; c) G. Suss-Fink, L. Plasseraud, V. Ferrand, S. Stanislas, A. Neels, H. Stoeckli-Evans, M. Henry, G. Laurenczy, R. Roulet, *Polyhedron* **1998**, *17*, 2817–2827.
[17] a) W. Schrimer, U. Florke, H.-J. Haupt, *Z. Anorg. Allg. Chem.* **1989**, *574*, 239–255; b) R. Mattes, K. Muhlsiepen, *Z. Naturforsch.* **1980**, *B35*, 265–268; c) E. W. Corcoran, Jr., *Inorg. Chem.* **1990**, *29*, 157–158; d) G. S. Kim, D. A. Keszler, C. W. DeKock, *Inorg. Chem.* **1991**, *30*, 574–577.
[18] C. D. Garner, J. M. Charnock, *In Comprehensive Coordination Chemistry, Vol. 3* (Eds.: G. Wilkinson, R. D. Gillard, J. A. McCleverty), Pergamon, Oxford, **1987**, pp. 1329–1374.
[19] Q. Chen, J. Zubieta, *Coord. Chem. Rev.* **1992**, 114, 107–167.
[20] I. D. Brown, D. Altermatt, *Acta Crystallogr. Sect. A* **1985**, *41*, 244–247.
[21] W. Liu, H. H. Thorp, *Inorg. Chem.* **1993**, *32*, 4102–4105.
[22] S. M. Kanowitz, G. J. Palenik, *Inorg. Chem.* **1998**, *37*, 2086–2089.
[23] J. C. J. Bart, V. Ragaini, *Inorg. Chim. Acta* **1979**, *36*, 261–265.
[24] L. Kihlborg, *Ark. Kemi.* **1963**, *21*, 471–495.
[25] W. H. Zachariasen, *J. Less-Common Met.* **1978**, *62*, 1–7.
[26] I. D. Brown, K. K. Wu, *Acta Crystallogr. Sect. B* **1976**, *32*, 1957–1959.
[27] R. Allmann, *Monatsh. Chem.* **1975**, *106*, 779–793.
[28] J. C. J. Bart, V. Ragaini, *Acta Crystallogr. Sect. B* **1980**, *36*, 1351–1354.
[29] I. D. Brown, *Structure and Bonding in Crystals*, Academic, New York, **1980**.
[30] G. Liu, Y.-G. Wei, J. Liu, Q. Liu, S.-W. Zhang, Y.-Q. Tang, *J. Chem Soc. Dalton Trans.* **2000**, 1013–1014.
[31] A. J. Millar, C. J. Doonan, L. J. Laughlin, E. R. T. Tiekink, C. G. Young, *Inorg. Chim. Acta* **2002**, *337*, 393–406.
[32] L. M. R. Hill, M. K. Taylor, V. W. L. Ng, C. G. Young, *Inorg. Chem.* in press.
[33] G. M. Sheldrick, *Programs for Crystal Structure Analysis (release 97–2)*, G. M. Sheldrick, Institüt für Anorganische Chemie der Universität, Tammanstrasse 4, D-3400 Göttingen, Germany, **1998**.

Received: November 9, 2007
Published online: January 23, 2008

